Position sensorless brushless DC motor/generator drives: review and future trends

T. Kim, H-W. Lee and M. Ehsani

Abstract: Recent advances in the development of fast digital signal processors (DSPs) have paved the way for position sensorless drives of alternating current motors. More sophisticated sensorless drive algorithms in DSPs substitute for the mechanical position sensors and other related hardware. The authors cover a wide range of topics related to the position sensorless control of brushless direct current motor/generator drives including their fundamentals, limitations, present advances and future trends. Conventional techniques are reviewed and recent developments in this area are introduced with their inherent advantages and drawbacks. Anticipated research efforts and trends are also discussed.

1 Introduction

The permanent magnet (PM) brushless DC (BLDC) motor offers many advantages including high efficiency, low maintenance, greater longevity, reduced weight and more compact construction. The BLDC motors have been widely used for various industrial applications based on their inherent advantages.

Recently, in an effort to replace existing hydraulic and pneumatic devices with electric actuators, many defense companies started using PM motors in military applications such as aircraft and gun turret drives for combat vehicles. As a result, the PM machine is increasingly being used for various military and commercial applications and its market is rapidly expanding.

However, the PM BLDC motors are inherently electronically controlled and require rotor position information for proper commutation of currents in its stator windings. For space-restricted applications such as aircrafts, the additional mechanical sensors increase the dimension of the PM machine drive and prohibit the use of the drive for such applications. In addition, it is not desirable to use the position sensors for applications where reliability is of utmost importance because a sensor failure causes control system instability. These limitations of using position sensors combined with the availability of powerful and economical microprocessors have spurred the development of sensorless control technology.

The brushless PM machines can be categorised based on the PMs mounting and shape of the back-EMF. The PMs can be surface mounted on the rotor or installed inside of the rotor (interior PM), and the back-EMF shape can either be sinusoidal or trapezoidal. The surface mounted PM (SMPM) BLDC machine has non-sinusoidal back-EMF waveforms due to the concentric winding of the machine and rectangular distribution of the magnetic flux in the air-gap. Typically, for this type of motor, the inductance variation by rotor position is negligibly small since there is no magnetic saliency. This machine is usually called the BLDC motor.

On the other hand, the interior permanent magnet (IPM) machine has an inductance variation by rotor position because of the magnetic saliency. The IPM machine is a good candidate for high-speed and traction applications. Fig. 1 illustrates structures of the SMPM BLDC and IPM machines.

The inductance variation of the IPM machine benefits sensorless operation. Therefore the sensorless operation for the BLDC machine has more limitation than that of the IPM machines. This paper will focus on the sensorless drive for the BLDC machines. In this paper, conventional and recent advancement of position sensorless drive methods for the PM BLDC motors and generators are presented. Also, expected future trends in this area are discussed.

2 Conventional sensorless drive technique for BLDC motors

For the BLDC motors, which have the SMPM structure, the Hall effect position sensors are usually used to identify which phase is to be commutated to maintain the electrical synchronism. For high performance drives, high-resolution optical encoders or resolvers are typically used. Various methods of sensorless operation for BLDC motors have been seen in the literature [1–55]. These sensorless drive techniques can be grouped into four categories:

1. Back-EMF based methods.
2. Flux calculation based methods.
3. Observer based methods.
4. Other methods.

doi:10.1049/iet-epa:20060358

Paper first received 14th September 2006 and in revised form 3rd February 2007

T. Kim is with the Electrical and Computer Engineering Department, University of Michigan-Dearborn, Dearborn, MI, USA

H-W. Lee is with the Signaling and Electrical Engineering Department, Korea Railroad Research Institute, Uiwang, South Korea

M. Ehsani is with the Electrical and Computer Engineering Department, Texas A&M University, College Station, TX, USA

E-mail: taehyung@umich.edu

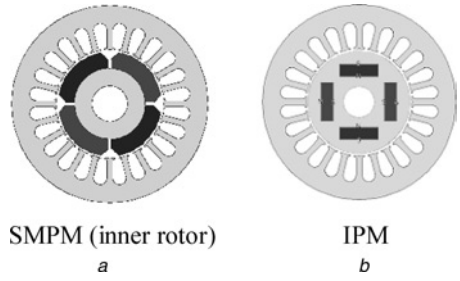

Fig. 1 *Structures of PM brushless motors*

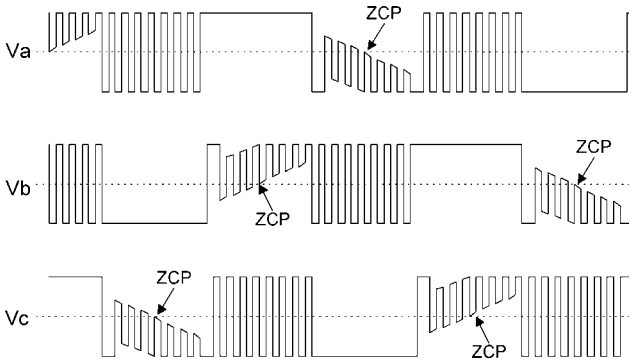

Fig. 3 *Measured terminal voltage waveform*

2.1 Back-EMF based methods

2.1.1 Based on the terminal voltage sensing: For typical operation of a BLDC motor, the phase current and back-EMF should be aligned to generate constant torque. The current commutation point shown in Fig. 2 can be estimated by the zero crossing point (ZCP) of back-EMFs and a 30° phase shift [1]. To detect the ZCPs, the phase back-EMF should be monitored during the silent phase. In [1], to monitor the phase back-EMF during the silent phase, the terminal voltages were low-pass filtered first. Three low-pass filters (LPFs) are utilised to eliminate higher harmonics caused by the inverter switching. Each output of the three filters on the terminal-to-motor neutral voltages is connected to a wye-connected resistive network. The time delay of LPFs will limit the high speed operation capability of the BLDC machine. At the point where a filtered terminal voltage crosses the neutral point voltage, back-EMF of that phase becomes zero and that point corresponds to the transition at the output of a comparator. Based on the comparator outputs phase currents are commutated.

On the other hand, in [2], the analogue LPFs are not utilised. Fig. 3 illustrates the measured terminal voltages when the unipolar pulse width modulation (PWM) scheme is used. The terminal voltages were sampled through the analogue-to-digital (A/D) converters only when the upper switch is on. The instance when the sampled values match with half of the DC link voltage is the ZCP of the back-EMF. Based on the time duration of present and previous zero crossings, the commutation instants are estimated. This method is applied for household air-conditioner compressor drives.

The drawback of the above methods is that it is not possible to use the noisy terminal voltage to obtain a switching pattern at low speeds since back-EMF is zero at standstill and proportional to rotor speed. Also, the estimated commutation points have position error during the transient period when the speed is accelerated or decelerated rapidly, especially for a system that has low inertia. With these methods, rotor position can be detected typically from 20% of the rated speed. Nevertheless, the terminal voltage sensing method is widely used for low cost industrial applications such as fans, pumps and compressor drives where frequent speed variation is not required.

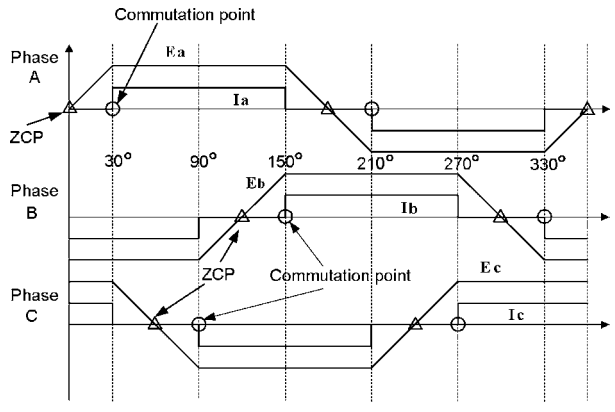

Fig. 2 *Zero crossing points of the back-EMFs and commutation points*

2.1.2 Based on the back-EMF integration: In this method, the commutation instant is determined by integration of the silent phase's back-EMF [3–6]. The basic idea of this method is that the integrated area of the back-EMFs shown in Fig. 4 is approximately the same at all speeds. The integration starts when the silent phase's back-EMF crosses zero. When the integrated value reaches a pre-defined threshold value, which corresponds to a commutation point, the phase current is commutated.

If flux weakening operation is required, current advance can be achieved by changing the threshold voltage. The integration approach is less sensitive to switching noise and automatically adjusts for speed changes, but low speed operation is poor due to the error accumulation and offset voltage problems from the integration.

2.1.3 Based on the third harmonic of the back-EMF sensing: This method utilises the third harmonic of the back-EMF to determine the commutation instants of the BLDC motors [7]. Since the third harmonic of the back-EMF has three times greater frequency, this method is not as sensitive to time delay of a LPF, which is a problem of the terminal voltage sensing method. The back-EMF terms can be represented using the Fourier

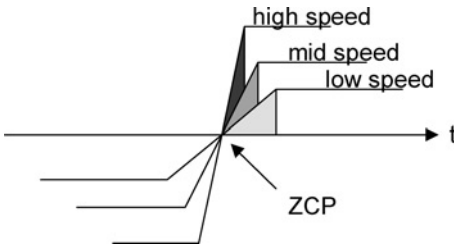

Fig. 4 *Integrated areas of the back-EMF*

expression as

$$
\begin{aligned}
e_a &= E_1 \sin\theta_r + E_3 \sin 3\theta_r + E_5 \sin 5\theta_r + \cdots \\
e_b &= E_1 \sin\left(\theta_r - \frac{2\pi}{3}\right) + E_3 \sin 3\left(\theta_r - \frac{2\pi}{3}\right) \\
&\quad + E_5 \sin 5\left(\theta_r - \frac{2\pi}{3}\right) + \cdots \\
e_c &= E_1 \sin\left(\theta_r - \frac{4\pi}{3}\right) + E_3 \sin 3\left(\theta_r - \frac{4\pi}{3}\right) \\
&\quad + E_5 \sin 5\left(\theta_r - \frac{4\pi}{3}\right) + \cdots
\end{aligned} \tag{1}
$$

Summing the three phase back-EMFs

$$
\begin{aligned}
e_a + e_b + e_c &= 3E_3 \sin 3\theta_r + 3E_9 \sin 9\theta_r + \cdots \\
&\simeq 3E_3 \sin 3\theta_r
\end{aligned} \tag{2}
$$

If each phase inductance is constant at any rotor position, from the summation of three-terminal to neural voltages, the third harmonic of the back-EMF can be measured as

$$
\begin{aligned}
V_{sum} &= v_{an} + v_{bn} + v_{cn} = \left(R + L\frac{d}{dt}\right)(i_a + i_b + i_c) \\
&\quad + (e_a + e_b + e_c) \\
&= e_a + e_b + e_c \simeq 3e_3 \sin 3\theta_r
\end{aligned} \tag{3}
$$

The summed terminal voltage includes only the triplent harmonics since the summation of the three phase currents is zero. Note that the third harmonic term dominates the summed voltage. Now, to obtain commutation instants, the summed voltage is integrated as (4).

$$
\lambda_{3rd} = \int V_{sum} dt \tag{4}
$$

As illustrated in Fig. 5, the zero crossings of the integrated third harmonic flux linkage are commutation points. To sense the third harmonic of the back-EMF, an external hardware circuit is required. The third harmonic-based method has a wider speed range and smaller phase delay than the terminal voltage sensing method. However, at low speed, the integration process can cause a serious position error, as noise and offset error from sensing can be accumulated for a relatively long period of time.

2.1.4 Based on the freewheeling diode conduction: This method utilises current flowing through a freewheeling diode in silent phase [8]. Right after the ZCP of the back-EMF in the silent phase, a tiny current is flowing through the freewheeling diode during the active phase switches are turned off under alternate chopper control. This silent phase current starts to flow approximately at the time where the back-EMF of the open phase crosses zero.

This method also has a position error of commutation points in the transient state as other back-EMF based methods. The most serious drawback of this method is the use of six isolated power supplies for the comparator circuitry to detect current flowing in each freewheeling diode. The drawback prohibits this method from practical applications.

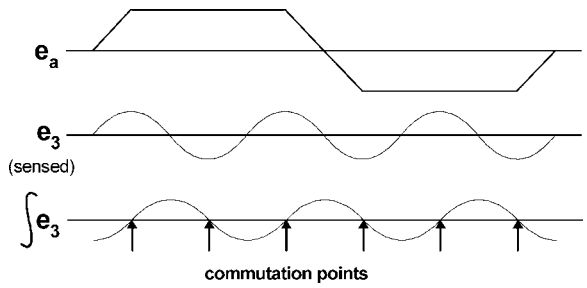

Fig. 5 *Third harmonic of the back-EMF and commutation points*

2.2 Flux calculation based methods

In this method, the flux linkage is estimated from measured voltages and currents and then the position is predicted by polynomial curve fitting [9, 10]. The fundamental idea is to take the voltage equation of the machine

$$
V = Ri + \frac{d}{dt}\lambda \tag{5}
$$

where V is the input voltage, i is the current, R is the resistance and λ is the flux linkage, respectively. Then, the flux linkage can be calculated as

$$
\lambda = \int_0^t (V - Ri)dt \tag{6}
$$

The rotor position can be estimated based on the initial position, machine parameters and relationship between the flux linkage and rotor position. At the very beginning of the integration the initial flux linkage has to be known precisely to estimate the next step flux linkages. This means that the rotor has to be at a known position at the start.

Fig. 6 shows the block diagram of the position estimation algorithm [10]. The current loop for current estimation 1 is used for prediction, estimation and the correction of the position. The other current loop for current estimation 2 is used for correction of the calculated flux linkage values.

This method also has an error accumulation problem for integration at low speeds. The method involves lots of computation and is sensitive to the parameter variation.

2.3 Observer-based methods

In this category, various types of observers are used to estimate rotor position. The fundamental idea is that a mathematical model of the machine is utilised and it takes measured inputs of the actual system and produces estimated outputs. Then, the error between the estimated outputs and measured quantities is fed back into the system model to correct the estimated values. The biggest advantage of using observers is that all of the states in the

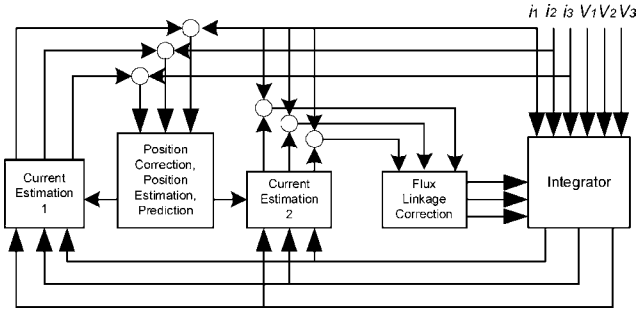

Fig. 6 *Schematic diagram of the flux linkage calculation based method [10]*

system model can be estimated including states that are hard to obtain by measurements.

Observers have been implemented in sensorless PM motor drive systems [11–33]. The reduced-order observers [13, 18] and disturbance observers [11, 12] are utilised to estimate back-EMFs. Also, sliding-mode observers are applied to estimate the rotor position utilising d and q axis stator currents [25–28].

Matsui described the method utilising the dq based mathematical model and measured dq currents and voltages [20, 21]. The error between the estimated dq voltages and measured dq voltages derives rotor position error, which is used to estimate rotor position and speed. The method cannot estimate rotor position at standstill and hence the forced alignment method is initially applied to lock the rotor in a desired position.

In [24], a similar model-based method is utilised for a surface-mounted PM machine that has negligibly small inductance variation. In this method, the error between measured dq currents and estimated dq currents based on the machine model is used to estimate rotor position and speed to drive a direct-drive washing machine. Since the parameter variation degrades the sensorless drive performance, the parameters are updated based on the temperature estimation. The temperature is estimated through a stator resistance when the motor speed is zero and the parameters are corrected based on the relationship between the temperature and parameters.

Most of the observer-based methods are used for PM AC motors, which have sinusoidal back-EMF and need continuous rotor position. Typically, for the BLDC motors, which require just six position points for one electrical cycle, the continuous position information from the observer is not necessary. But, for special purposes such as flux weakening operation based on advanced angle control, the positions between commutation points will be required.

2.4 Other methods

Two popular methods not mentioned in the previous three categories are the signal injection method and inductance-based method. These two methods are sometimes utilised together. The inductance-based method is popular for a motor that has severe saliency such as switched reluctance motors and interior PM motors.

In most cases, from fundamental motor voltage equations, the inductance is calculated based on other measured quantities. In [34], to detect rotor position at standstill, a diagnostic current is injected. Based on the current, the rotor pole sign is estimated. This method detects the difference of the saturation level based on the sign of rotor magnet flux. Two voltage pulses with opposite signs are applied for a predetermined time for the purpose. Then, maximum current is measured at the end of the applied voltage pulse. The difference between the positive and negative maximum currents is calculated to find out which pole is close to the corresponding phase. For other phases, the same procedure is repeated. The resultant three signs provide information regarding which phase should be excited first. This method provides 60º (electrical) resolution at standstill.

A similar approach is done in [35] to detect the rotor position at standstill. If there is a sufficient magnetic saturation-level difference when a different PM pole is located, the rotor pole can be identified at standstill by applying positive and negative voltage pulses and measuring magnitude of the resultant current.

In [36–38], a high-frequency signal is injected to detect inductance, which is a function of rotor position for salient PM motors. Once there is a significant magnetic saliency in the motor, the initial rotor position at standstill can be detected based on the incremental inductance calculation [39–41].

In [42], to create artificial saliency, a thin non-magnetic material is attached to the round surface of the PMs. In this case, the stator inductance changes with rotor position as the eddy currents in the aluminium act to decrease the inductance. By applying rectangular voltage pulses and measuring the maximum current amplitudes, the position can be estimated. However, the additionally attached non-magnetic material can increase the air-gap of the motor, and hence can decrease the efficiency.

In [43, 44], the DC bus current shape is used to estimate commutation error. When the motor phase current is not synchronised with the back-EMF, the DC bus current is distorted. Based on the DC bus current observation, when the phase current leads and lags the back-EMF, DC link input voltage is updated to align the current and back-EMF, and continuously maintains the synchronism of the motor.

3 Recent advancements in sensorless BLDC motor drives

In many practical applications for non-salient, surface mounted BLDC motors, the back-EMF based methods are commonly utilised to estimate the rotor position. These back-EMF based methods show good performance above a certain speed but suffer at low speeds since the back-EMF voltage is proportional to speed. Therefore the performance of the most conventional sensorless drive methods is degraded in low speeds and the rotor position cannot be detected at standstill if there is no significant saliency. In this section, recent advancements in the sensorless BLDC motor drives will be introduced based on the literature published after year 2000.

In [45], the terminal voltage sensing method is applied for an automotive application. Unlike conventional vehicles that use a belt to drive air conditioner compressors, hybrid electric vehicles use an electric compressor, which is independent from the engine. Because of the requirement of sealing and cost, sensorless drive is integrated in the semi-integrated packaging compressor drive. A well-known sensorless controller chip, ML4425 (Fairchild), is utilised based on the terminal voltage sensing. Sensorless commutation is achieved by means of a phase-lock loop (PLL). Speed ranges from 600 to 6000 rpm without position sensors is reported for a 42-V automotive compressor drive.

In [46], a low-cost version of the terminal voltage sensing method is applied for applications that do not require rapid acceleration or deceleration. Only one terminal voltage is sensed and goes through an integrator to detect zero crossings. The time interval of zero crossings, T_k, corresponds to 180° by electrical angle. Therefore $T_k/3$ will be the commutation interval. Based on the interpolation, six-step commutation instants are decided. The simplified terminal voltage sensing method will be limited to apply only for applications where speed variation is not frequently required.

For terminal voltage detection methods, LPFs are typically used causing phase delays. In the conventional ZCP detection methods, noisy terminal voltages pass through LPFs first and they are compared with a threshold value using a comparator to detect back-EMF zero crossings. In [47], authors do not utilise LPFs to avoid unwanted phase delays. Since no LPF is used, the comparator output signal includes false zero crossings. Therefore a predefined

logic operation is used instead of analogue LPFs to digitally eliminate the false zero crossings. With the method, high speed ranges of sensorless BLDC drives can be extended compared to conventional zero crossing detection methods which use the LPF.

The improved version of the third harmonic voltage sensing method is also reported using a PLL [48]. Authors have focused on the freewheeling diode conduction period right after the commutation. The inverted terminal voltage measured during the diode conduction period causes position error because of the unbalanced integration. Authors inverted the measured terminal voltage during the diode conduction period to decrease the commutation angle error. The method can be integrated into the ML4425 application-specific integrated circuit. Around 5% power loss improvement is reported at 120 k rpm with this method.

For all signal injection-based methods, a certain amount of saliency is required to detect rotor position. Thus, the high frequency signal injection method is straightforward for salient PM motors having rotors with buried or inset PMs. However, recently, several high-frequency injection methods with improved performance for small saliency PM motors are reported [49, 50].

In [49], the high-frequency impedance difference between the d and q axes of a BLDC motor is used to detect rotor position. With this method, low speed sensorless operation, including standstill, is reported. The method is applied for a surface-mounted PM BLDC motor, which usually has very small saliency. The small impedance variation, due to the magnetic saliency, is amplified through the injected high-frequency voltage.

When the injection frequency is sufficiently higher than the rotor speed of the BLDC motor, the high-frequency components of the voltage equation [49] can be given as

$$\begin{bmatrix} v^{\mathrm{r}}_{d\mathrm{sh}} \\ v^{\mathrm{r}}_{q\mathrm{sh}} \end{bmatrix} = \begin{bmatrix} r_{d\mathrm{h}} + L_{d\mathrm{h}}p & 0 \\ 0 & r_{q\mathrm{h}+L_{q\mathrm{h}}p} \end{bmatrix} \begin{bmatrix} i^{\mathrm{r}}_{d\mathrm{sh}} \\ i^{\mathrm{r}}_{q\mathrm{sh}} \end{bmatrix} \tag{7}$$

where $v^{\mathrm{r}}_{d\mathrm{sh}}$ and $i^{\mathrm{r}}_{q\mathrm{sh}}$ are d axis high-frequency voltage and current in the actual synchronous reference frame, respectively. $L_{d\mathrm{h}}$ and $r_{d\mathrm{h}}$ are d axis inductance and resistance at the injected high frequency, respectively. Then, authors utilised the modified high-frequency voltage equation in steady-state as

$$\begin{aligned} \begin{bmatrix} v^{\mathrm{r}}_{d\mathrm{sh}} \\ v^{\mathrm{r}}_{q\mathrm{sh}} \end{bmatrix} &= \begin{bmatrix} r_{d\mathrm{h}} + j\omega_{\mathrm{h}}L_{d\mathrm{h}} & 0 \\ 0 & r_{q\mathrm{h}} + j\omega_{\mathrm{h}}L_{q\mathrm{h}} \end{bmatrix} \begin{bmatrix} i^{\mathrm{r}}_{d\mathrm{sh}} \\ i^{\mathrm{r}}_{q\mathrm{sh}} \end{bmatrix} \\ &\equiv \begin{bmatrix} z^{\mathrm{r}}_{d\mathrm{h}} & 0 \\ 0 & z^{r}_{q\mathrm{h}} \end{bmatrix} \begin{bmatrix} i^{\mathrm{r}}_{d\mathrm{sh}} \\ i^{\mathrm{r}}_{q\mathrm{sh}} \end{bmatrix} \end{aligned} \tag{8}$$

where $z^{\mathrm{r}}_{d\mathrm{h}}$ and ω_{h} are d axis high-frequency impedance and injected frequency, respectively. Equation (8) can be transformed to the estimated synchronous reference frame considering the rotor position estimation error as

$$\begin{bmatrix} \hat{v}^{\mathrm{r}}_{d\mathrm{sh}} \\ \hat{v}^{\mathrm{r}}_{q\mathrm{sh}} \end{bmatrix} = \begin{bmatrix} z_{\mathrm{avg}} + \frac{1}{2}z_{\mathrm{diff}}\cos 2\tilde{\theta}_{\mathrm{r}} & \frac{1}{2}z_{\mathrm{diff}}\sin 2\tilde{\theta}_{\mathrm{r}} \\ \frac{1}{2}z_{\mathrm{diff}}\sin 2\tilde{\theta}_{\mathrm{r}} & 2z_{\mathrm{avg}} - \frac{1}{2}z_{\mathrm{diff}}\cos 2\tilde{\theta}_{\mathrm{r}} \end{bmatrix} \begin{bmatrix} \hat{i}^{\mathrm{r}}_{d\mathrm{sh}} \\ \hat{i}^{\mathrm{r}}_{q\mathrm{sh}} \end{bmatrix} \tag{9}$$

where, $\tilde{\theta}_{\mathrm{r}}$, z_{avg} and z_{diff}, are the rotor position estimation error, the average of d and q axes high-frequency impedances and the difference between d and q axes high-frequency impedances, respectively. When the high-frequency voltage is injected on the d-axis only, the resultant d and q axes high-frequency currents contain the indication of rotor position estimation error as

$$\begin{aligned} \hat{i}^{\mathrm{r}}_{d\mathrm{sh}} &= \frac{V_{\mathrm{inj}}\cos\omega_{\mathrm{h}}t}{z^{\mathrm{r}}_{d\mathrm{h}}z^{\mathrm{r}}_{q\mathrm{h}}}\left(z_{\mathrm{avg}} - \frac{1}{2}z_{\mathrm{diff}}\cos 2\tilde{\theta}_{\mathrm{r}}\right) \\ \hat{i}^{\mathrm{r}}_{q\mathrm{sh}} &= \frac{V_{\mathrm{inj}}\cos\omega_{\mathrm{h}}t}{z^{\mathrm{r}}_{d\mathrm{h}}z^{\mathrm{r}}_{q\mathrm{h}}}\left(-\frac{1}{2}z_{\mathrm{diff}}\sin 2\tilde{\theta}_{\mathrm{r}}\right) \end{aligned} \tag{10}$$

where L_{diff} is the difference between the d and q axes inductances at high frequency. Since the q axis high-frequency current becomes zero when the estimated position is zero, the q axis high-frequency current shown in (10) is utilised to estimate the rotor position.

The final equation for the position estimation is as follows

$$i_{\tilde{\theta}_{\mathrm{r}}} \equiv \mathrm{LPF}(\hat{i}^{\mathrm{r}}_{q\mathrm{sh}}\sin\omega_{\mathrm{h}}t) = -\frac{V_{\mathrm{inj}}L_{\mathrm{diff}}}{4\omega_{\mathrm{h}}L_{d\mathrm{h}}L_{q\mathrm{h}}}\sin 2\tilde{\theta}_{\mathrm{r}} \tag{11}$$

To calculate the input signal ($i_{\tilde{\theta}_{\mathrm{r}}}$) of the rotor position estimator, a band-pass filter, a multiplication and a LPF are used as illustrated in Fig. 7.

The standstill position detection with four quadrant sensorless operation is reported with this method. However, this method utilises the high-frequency voltage that has fairly high magnitude (above 40 V) to detect high-frequency impedance differences. Therefore non-negligible harmonic loss is expected. To utilise the method, the motor back iron should be properly designed to generate the appropriate level of local saturation.

The updated method from [49] is reported without high-frequency signal injection [51]. The authors utilise a rotor position tracking PI controller to estimate the rotor speed, which is used to control the rotor position error to zero. The PI controller gain has a variable structure for zero and low-speed operation.

In [52], a speed-independent position function that is based on two flux linkage functions is utilised. One of the advantages of this method is that the instantaneous speed term, which is hard to obtain, is eliminated to estimate commutation points. This feature makes the method have better performance at low speeds and transient state.

The speed independent characteristic provides an advantage to detect commutation instants, especially in transient state when the rotor speed is rapidly changed with low inertia. However, the method also suffers from a lack of standstill as well as near zero speed position detection.

In [53], a sensorless drive method using a matrix converter is reported. The authors adopt an existing high-frequency voltage injection method to highlight the inherent advantage of applying the matrix converter to sensorless drives. Under regular voltage source inverter with PWM, the measured quantities (especially terminal voltage) are highly non-linear and need filtering.

On the other hand, the matrix converter can provide almost linear relationship between the demanded and

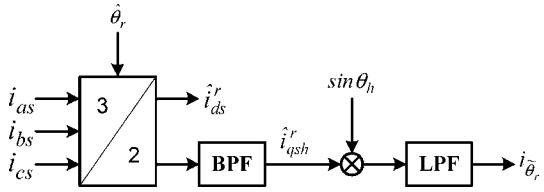

Fig. 7 *Position detection procedure to calculate the $i_{\tilde{\theta}_r}$ [49]*

actual output voltages. The converter linearity can bring advantages for existing sensorless methods especially at the low speed region. Although the matrix converter is utilised with a signal-injection method for a small saliency motor, the characteristic of the matrix converter can benefit other existing sensorless drive methods, which suffer at low speeds. However, in practice, the higher system cost of the matrix converter will limit its use for low-cost sensorless drive applications, which represents most cases. Also, the output voltage limitation (around 86% of the input voltage) of matrix converters will reduce the power density of the system.

4 Position sensorless BLDC generator drives

The SMPM BLDC machine has the trapezoidal back-EMF waveform [56, 57]. Because of the difference of the back-EMF waveform, non-sinusoidal BLDC generators can have around 15% higher power density compared with a PM synchronous generator, which has the sinusoidal back-EMF [58]. With the inherent advantages of a BLDC generator, additional increases in power density and efficiency can be expected by advanced control schemes, resulting in considerable reduction of weight and volume of the machine.

Conventionally, the full-bridge diode rectifier is used for power generation of a BLDC generator because of several advantages such as low cost and simple control. However, it has a poor power factor and a low power per ampere ratio [59, 60].

In a sinusoidal power supply system such as a PM synchronous generator, generally, a PWM rectifier is used for power factor correction [61–63]. With given sinusoidal current references, six active switches can control the current to be in phase with voltage of the generator. In this case, a position sensor is required to synchronise current with generated voltages. For the BLDC generator, which is a non-sinusoidal power supply system, the optimal current waveform for maximum power density and efficiency is not sinusoidal and the same control scheme for sinusoidal PWM rectifier cannot be used to achieve maximum output power.

In [64, 65], the optimal current waveform is calculated based on the simple algebraic method without using the complicated fast Fourier transform. This method utilises calculated line-to-line back-EMFs in real time to calculate optimal current waveform, and hence the position sensors are not required.

In [65], authors proved that the maximum power density in the non-sinusoidal machine is accomplished by matching all of the harmonics of current with those of the induced EMF, except zero-sequence harmonics. To calculate the optimal current waveform in real time, line-to-line back-EMFs are calculated, and based on the unique equation, zero-sequence harmonics are eliminated.

Each phase EMF has harmonics and the sum of phase EMFs can be categorised by the zero and zero-sequence component as in (12) and (13) for an N phase machine. The zero-sequence harmonics are identical for any phase as in (14). By substituting (14) into (12), the components that do not include the zero-sequence can be derived in (15).

$$e_{\mathrm{a}} = e_{\mathrm{a1}} + e_{\mathrm{a3}} + e_{\mathrm{a5}} + \cdots = e_{am} + e_{\mathrm{az}}\ (z = N_m^{\mathrm{th}}\text{harmonics}) \tag{12}$$

$$e_{\mathrm{a}} + e_{\mathrm{b}} + \cdots + e_N = \underbrace{e_{am} + e_{\mathrm{b}m} + \cdots + e_{Nm}}_{0} + \underbrace{e_{\mathrm{az}} + e_{\mathrm{bz}} + \cdots + e_{Nz}}_{\text{zerosequence}} \tag{13}$$

$$e_{\mathrm{az}} = e_{\mathrm{bz}} = \cdots = e_{\mathrm{cz}} = e_z \Rightarrow e_z = \frac{1}{N}(e_{\mathrm{a}} + e_{\mathrm{b}} + \cdots + e_N) \tag{14}$$

$$e_{am} = e_{\mathrm{a}} - e_z = e_{\mathrm{a}} - \frac{1}{N}(e_{\mathrm{a}} + e_{\mathrm{b}} + \cdots + e_N)$$

$$e_{\mathrm{b}m} = e_{\mathrm{b}} - e_z = e_{\mathrm{b}} - \frac{1}{N}(e_{\mathrm{a}} + e_{\mathrm{b}} + \cdots + e_N) \tag{15}$$

$$\vdots$$

$$e_{Nm} = e_N - e_z = e_N - \frac{1}{N}(e_{\mathrm{a}} + e_{\mathrm{b}} + \cdots + e_N)$$

Then, the optimal current reference for N phase BLDC generators is derived as (16).

$$[i_N^*] = g \cdot \frac{1}{N} \underbrace{\begin{bmatrix} N-1 & -1 & \cdots & \cdots & -1 \\ -1 & \ddots & & & \vdots \\ \vdots & & \ddots & & \vdots \\ \vdots & & & \ddots & -1 \\ -1 & \cdots & \cdots & -1 & N-1 \end{bmatrix}}_{N} \times \begin{bmatrix} e_{\mathrm{a}} \\ e_{\mathrm{b}} \\ e_{\mathrm{c}} \\ \vdots \\ e_N \end{bmatrix} \tag{16}$$

where, g is a proportional gain from the output voltage controller and N is the number of phases. The advantage of the method is that the optimal current equation, (16) can be further derived by line-to-line back-EMFs instead of the phase to neutral back-EMFs. With this method, it is reported that around 40% of the power is increased compared to the diode rectifier generation system.

5 Future trends

Several Asian countries such as Japan, which has been under pressure from high energy prices, have implemented the variable speed PM motor drives for energy saving applications such as air conditioners and refrigerators since the past two decades [1]. On the other hand, the US has kept on using cheap induction motor drives, which have around 10% lower efficiency than adjustable PM motor drives for energy saving applications. Therefore recently, the pain of energy prices for customers spurs higher demands of variable speed PM motor drives. Also, recent rapid proliferation of motor drives into the automobile industry, based on the hybrid synergy drives, generates a serious demand for high efficient PM motor drives.

Based on all these driving factors, various sensorless drive schemes for BLDC motors will open the way for full penetration of the BLDC motor drive into various military and commercial applications.

Recently, the microprocessor technology has shown incredible improvements and the operating speed of DSPs has been faster and faster. Complicated control algorithms can now be easily implemented in a DSP with high sampling and calculation frequency. The existing sensorless

drive techniques can be greatly improved utilising many of the recent advancements in DSPs.

As addressed, in the most recent sensorless drive methods, rotor position is estimated based on motor parameters and measured quantities. Since significant BLDC motor parameter variation can occur by mass production, motor aging and temperature variation during operation, the sensorless drive technique, with self-tuning, which can compensate parameter variations, is required.

Optimal performance of BLDC machine drive cannot be achieved with a control-method based on the rotor position obtained from a position sensor such as encoders or Hall sensors that are insensitive to parameter variation. New fast DSPs for motor drives can handle more complicated control algorithms including the online parameter tuning. Also, adapting the artificial intelligence control such as neural network and fuzzy logic is more practical nowadays due to the faster DSP chips [66–68]. The combination of advanced DSP technology and sophisticated control will yield a better sensorless BLDC drive that has higher performance than even conventional motor drives with position Hall sensors in the near future.

6 Conclusions

In this paper, a review of position sensorless drives for BLDC motors and generators has been presented. The fundamentals of various methods have been introduced as a useful reference for preliminary investigation of conventional methods. The recent advances in the position sensorless control and the expected future research works were also discussed.

To provide insight in sensorless drive techniques and their benefits, classification of existing sensorless methods and newer methods were presented with their merits and drawbacks. From the above discussion, it is obvious that the sensorless control for BLDC motors and generators can be utilised in a greater variety of applications requiring higher performance. Further research is required such as online self-tuning without position sensors to realise optimal performance.

7 References

1 Iizuka, K., Uzuhashi, H., and Kano, M.: 'Microcomputer control for sensorless brushless motor', *IEEE Trans. Ind. Appl.*, 1985, **IA-27**, pp. 595–601

2 Hong, C.S., Yeo, H.G., Yoo, J.Y., Bae, Y.D., and Park, Y.S.: 'Sensorless drive for interior permanent magnet brushless DC motors'. IEEE IEMDC Conf., 1997, pp. TD1/3.1–TD1/3.3

3 Becerra, R.C., Jahns, T.M., and Ehsani, M.: 'Four-quadrant sensorless brushless ECM drive'. IEEE APEC Conf., 1991, pp. 202–209

4 Jahns, T.M., Becerra, R.C., and Ehsani, M.: 'Integrated current regulation for a brushless ECM drive', *IEEE Trans. Power Electron.*, 1991, **6**, pp. 118–126

5 Regnier, D., Oudet, C., and Prudham, D.: 'Starting brushless DC motors utilizing velocity sensors'. Proc. Incremental Motion Control Systems and Devices, 1985, pp. 99–107

6 Peters, D., and Harth, J.: 'ICs provide control for sensorless DC motors'. Proc. EDN, 1993, pp. 85–94

7 Moreira, J.: 'Indirect sensing for rotor flux position of permanent magnet AC motors operating in a wide speed range', *IEEE Trans. Ind. Appl.*, 1996, **32**, pp. 401–407

8 Ogasawara, S., and Akagi, H.: 'An approach to position sensorless drive for brushless DC motors', *IEEE Trans. Ind. Appl.*, 1991, **27**, pp. 928–933

9 Ertugrul, N., Acarnley, P.P., and French, C.D.: 'Real-time estimation of rotor position in PM motors during transient operation'. IEE Conf., 1993, pp. 311–316

10 Ertugrul, N., and Acarnley, P.: 'A new algorithm for sensorless operation of permanent magnet motors', *IEEE Trans. Ind. Appl.*, 1994, **30**, pp. 126–133

11 Senjyu, T., and Uezato, K.: 'Adjustable speed control of brushless DC motors without position and speed sensors'. IEEE IAS Conf., 1995, pp. 160–164

12 Senjyu, T., Tomita, M., Doki, S., and Okuma, S.: 'Sensorless vector control of brushless DC motors using disturbance observer'. IEEE PESC Conf., 1995, vol. 2, pp. 772–777

13 Kim, J., and Sul, S.: 'High performance PMSM drives without rotational position sensors using reduced order observer'. IEEE IAS Conf., 1995, vol. 1, pp. 75–82

14 Hu, J., Zhu, D., Li, Y., and Gao, J.: 'Application of sliding observer to sensorless permanent magnet synchronous motor drive system'. IEEE PESC Conf., 1994, vol. 1, pp. 532–536

15 Consoli, A., Musumeci, S., Raciti, A., and Testa, A.: 'Sensorless vector and speed control of brushless motor drives', *IEEE Trans. Ind. Electron.*, 1994, **41**, pp. 91–96

16 Sepe, R.B., and Lang, J.H.: 'Real-time observer-based (adaptive) control of a permanent-magnet synchronous motor without mechanical sensors', *IEEE Trans. Ind. Appl.*, 1992, **28**, pp. 1345–1352

17 Sicot, L., Siala, S., Debusschere, K., and Bergmann, C.: 'Brushless DC motor control without mechanical sensors'. IEEE PESC Conf., 1996, vol. 1, pp. 375–380

18 Solsona, J., Valla, M.I., and Muravchik, C.: 'A nonlinear reduced order observer for permanent magnet synchronous motors', *IEEE Trans. Ind. Electron.*, 1996, **IE-43**, pp. 492–497

19 Solsona, J., Valla, M.I., and Muravchik, C.: 'On speed and rotor position estimation in permanent-magnet AC drives', *IEEE Trans. Ind. Electron.*, 2000, **IE-47**, pp. 1176–1180

20 Matsui, N., and Shigyo, M.: 'Brushless dc motor control without position and speed sensors', *IEEE Trans. Ind. Appl.*, 1992, **IA-28**, pp. 120–127

21 Matsui, N.: 'Sensorless PM brushless DC motor drives', *IEEE Trans. Ind. Electron.*, 1996, **IE-43**, pp. 300–308

22 Takeshita, T., Usui, A., and Matsui, N.: 'Sensorless salient-pole PM synchronous motor drive in all speed ranges', *Electr. Eng. Jpn*, 2001, **135**, (3), pp. 64–73

23 Nahid-Mobarakeh, B., Meibody-Tabar, F., and Sargos, F.-M.: 'Mechanical sensorless control of PMSM with online estimation of stator resistance', *IEEE Trans. Ind. Appl.*, 2004, **IA-40**, pp. 457–471

24 Cho, K.Y., Yang, S.B., and Hong, C.H.: 'Sensorless control of a PM synchronous motor for direct drive washer without rotor position sensors', *IEE Proc.*, 2004, **151**, pp. 61–69

25 Kim, Y., Ahn, J., You, W., and Cho, K.: 'A speed sensorless vector control for brushless DC motor using binary observer'. IEEE IECON Conf., 1996, vol. 3, pp. 1746–1751

26 Furuhashi, T., Sangwongwanich, S., and Okuma, S.: 'A position-and-velocity sensorless control for brushless DC motors using an adaptive sliding mode observer', *IEEE Trans. Ind. Electron.*, 1992, **39**, pp. 89–95

27 Peixoto, Z., and Seixas, P.: 'Application of sliding mode observer for induced e.m.f., position and speed estimation of permanent magnet motors'. IEEE IECON Conf., 1995, pp. 599–604

28 Chen, Z., Tomita, M., Doki, S., and Okuma, S.: 'New adaptive sliding observers for position- and velocity-sensorless controls of brushless DC motors', *IEEE Trans. Ind. Electron.*, 2000, **47**, (3), pp. 582–591

29 Lee, K.-W., Jung, D.-H., and Ha, I.-J.: 'An online identification method for both stator resistance and back-EMF coefficients of PMSMs without rotational transducers', *IEEE Trans. Ind. Electron.*, 2004, **51**, pp. 507–510

30 Andreescu, G.D.: 'Adaptive observer for sensorless control of permanent magnet synchronous motor drives', *Electr. Power Compon. Syst.*, 2002, **30**, pp. 107–119

31 Schroedl, M.: 'Digital implementation of a sensorless control algorithm for permanent magnet synchronous motors'. Proc. Int. Conf. on "SM 100", ETH Zurich, 1991, pp. 430–435

32 Schroedl, M.: 'Operation of the permanent magnet synchronous machine without a mechanical sensor'. Proc. Int. Conf. on Power Electronics and Variable-Speed Drives, July 1990, pp. 51–56

33 Brunsbach, B.J., Henneberger, G., and Klepsch, T.: 'Position controlled permanent magnet excited synchronous motor without mechanical sensors'. IEE Conf., 1993, vol. 6, pp. 38–43

34 Schmidt, P., Gasperi, M., Ray, G., and Wijenayake, A.H.: 'Initial rotor angle detection of a non-salient pole permanent-magnet synchronous motor drive'. in Conf. Rec. IEEE IAS Conf., 1997, vol. 1, pp. 459–463

35 Nakashima, S., Inagaki, Y., and Miki, I.: 'Sensorless initial rotor position estimation of surface permanent-magnet synchronous motor', *IEEE Trans. Ind. Appl.*, 2000, **36**, pp. 1598–1603

36 Noguchi, T., Yamada, K., Kondo, S., and Takahashi, I.: 'Initial rotor position estimation method of sensorless PM synchronous motor with no sensitivity to armature resistance', *IEEE Trans. Ind. Electron.*, 1998, **45**, pp. 118–125

37 Aihara, T., Toba, A., Yanase, T., Mashimo, A., and Endo, K.: 'Sensorless torque control of salient-pole synchronous motor at zero-speed operation', *IEEE Trans. Power Electron.*, 1999, **14**, pp. 202–208

38 Haque, M.E., Zhong, L., and Rahman, M.F.: 'A sensorless initial rotor position estimation scheme for a direct torque controlled interior permanent magnet synchronous motor drive', *IEEE Trans. Power Electron.*, 2003, **18**, pp. 1376–1383

39 Ostlund, S., and Brokemper, M.: 'Sensorless rotor position detection from zero to rated speed for an integrated PM synchronous motor drive', *IEEE Trans. Ind. Appl.*, 1996, **32**, pp. 1158–1165

40 Jang, G., Park, J., and Chang, J.: 'Position detection and start-up algorithm of a rotor in a sensorless BLDC motor utilizing inductance variation', *IEE Proc.*, 2002, **149**, pp. 137–142

41 Tursini, M., Petrella, R., and Parasiliti, F.: 'Initial rotor position estimation method for PM motors', *IEEE Trans. Ind. Appl.*, 2003, **39**, pp. 1630–1640

42 Tomita, M., Satoh, M., Yamaguchi, H., Doki, S., and Okuma, S.: 'Sensorless estimation of rotor position of cylindrical brushless DC motors using eddy current'. IEEE Int. Workshop on Advanced Motion Control, 1996, pp. 24–28

43 Frederiksen, P.S., Birk, J., and Blaabjerg, F.: 'Comparison of two energy optimizing techniques for PM-machines'. IEEE IECON Conf., 1994, pp. 32–37

44 Johnson, J.P.: 'Synchronous-misalignment detection/correction technique of sensorless BLDC control'. Ph.D thesis, Texas A&M University, 1998

45 Naidu, M., Nehl, T.W., Gopalakrishnan, S., and Wurth, L.: 'Keeping cool while saving space and money: a semi-integrated, sensorless PM brushless drive for a 42-V automotive HVAC compressor', *IEEE Ind. Appl. Mag.*, 2005, **11**, (4), pp. 20–28

46 Su, G.-J., and Mckeever, J.W.: 'Low-cost sensorless control of brushless DC motors with improved speed range', *IEEE Trans. Power Electron.*, 2004, **19**, (2), pp. 296–302

47 Jiang, Q., Bi, C., and Huang, R.: 'A new phase-delay-free method to detect back EMF zero-crossing points for sensorless control of spindle motors', *IEEE Trans. Magn.*, 2005, **41**, (7), pp. 2287–2294

48 Shen, J.X., and Iwasaki, S.: 'Sensorless control of ultrahigh-speed PM brushless motor using PLL and third harmonic back EMF', *IEEE Trans. Ind. Electron.*, 2006, **53**, (2), pp. 421–428

49 Jang, J., Sul, S., Ha, J., Ide, K., and Sawamura, M.: 'Sensorless drive of surface-mounted permanent-magnet motor by high-frequency signal injection based on magnetic saliency', *IEEE Trans. Ind. Appl.*, 2003, **39**, (4), pp. 1031–1039

50 Linke, M., Kennel, R., and Holtz, J.: 'Sensorless position control of permanent magnet synchronous machines without limitation'. IEEE IECON Conf., Seville, Spain, November 2002, vol. 1, pp. 674–679

51 Seok, J.-K., Lee, J.-K., and Lee, D.-C.: 'Sensorless speed control of nonsalient permanent-magnet synchronous motor using rotor-position-tracking PI controller', *IEEE Trans. Ind. Electron.*, 2006, **53**, (2), pp. 399–405

52 Kim, T., and Ehsani, M.: 'Sensorless control of the BLDC motors from near zero to high speed', *IEEE Trans. Power Electron.*, 2004, **19**, (6), pp. 1635–1645

53 Arias, A., Silva, C.A., Asher, G.M., Clare, J.C., and Wheeler, P.W.: 'Use of a matrix converter to enhance the sensorless control of a surface-mount permanent-magnet AC motor at zero and low frequency', *IEEE Trans. Ind. Electron.*, 2006, **53**, (2), pp. 440–449

54 Bianchi, N., Bolognani, S., and Sul, S.K.: 'Comparison of PM motor structures and sensorless control techniques for zero-speed rotor position detection'. IEEE PESC Conf., July 2006, pp. 1821–1827

55 Ohto, M., and Sul, S.K.: 'Design and selection of AC machines for saliency-based sensorless control'. IEEE IAS Conf., October 2002, pp. 1155–1162

56 Hendershot, J.R. Jr., and Miller, T.J.E. (Oxford Magna Physics Publications 'Design of brushless permanent-magnet motors'. ISBN 1-881855-03-1, 1994

57 Mohan, N., Undeland, T.M., and Robbins, W.P.: 'Power electronics: converters, applications and design' (John Wiley & Sons, 1995, 2nd edn.)

58 Krishnan, R., and Rim, G.H.: 'Modeling, simulation, and analysis of variable-speed constant frequency power conversion scheme with a permanent magnet brushless DC generator', *IEEE Trans. Ind. Electron.*, 1990, **37**, (4), pp. 291–296

59 Bose, B.K.: 'Power electronics—a technology review', *Proc. IEEE*, 1992, **80**, (8), pp. 1303–1334

60 Lim, J.W., and Kwon, B.H.: 'A power-factor controller for single-phase PWM rectifiers', *IEEE Trans. Ind. Electron.*, 1999, **46**, (5), pp. 1035–1037

61 Martinez, R., and Enjeti, P.N.: 'A high-performance single-phase rectifier with input power factor correction', *IEEE Trans. Power Electron.*, 1996, **11**, (2), pp. 311–317

62 Stihi, O., and Ooi, B.T.: 'A single-phase controlled-current PWM rectifier', *IEEE Trans. Power Electron.*, 1988, **3**, (4), pp. 453–459

63 Boys, J.T., and Green, A.W.: 'Current-forced single-phase reversible rectifier', *IEE Proc.*, 1989, **136**, (5), pp. 205–211

64 Lee, H.-W., Kim, T., and Ehsani, M.: 'Practical control for improving power density and efficiency of the BLDC generator', *IEEE Trans. Power Electron.*, 2005, **20**, (1), pp. 192–199

65 Lee, H.-W., Kim, T., and Ehsani, M.: 'Maximum power throughput in the multiphase BLDC generator', *IEE Proc.*, 2005, **152**, pp. 2491–2496

66 Bose, B.K.: 'Fuzzy logic and neural networks in power electronics and drives', *IEEE Ind. Appl. Mag.*, 2000, **6**, pp. 57–63

67 Bose, B.K.: 'Artificial neural network applications in power electronics'. IEEE IECON Conf., 2001, vol. 3, pp. 1631–1638

68 Bose, B.K.: 'Technology advancement and trends in power electronics'. IEEE IECON Conf., 2003, vol. 3, pp. 3019–3020